Fessing et al., http://www.jcb.org/cgi/content/full/jcb.201101148/DC1

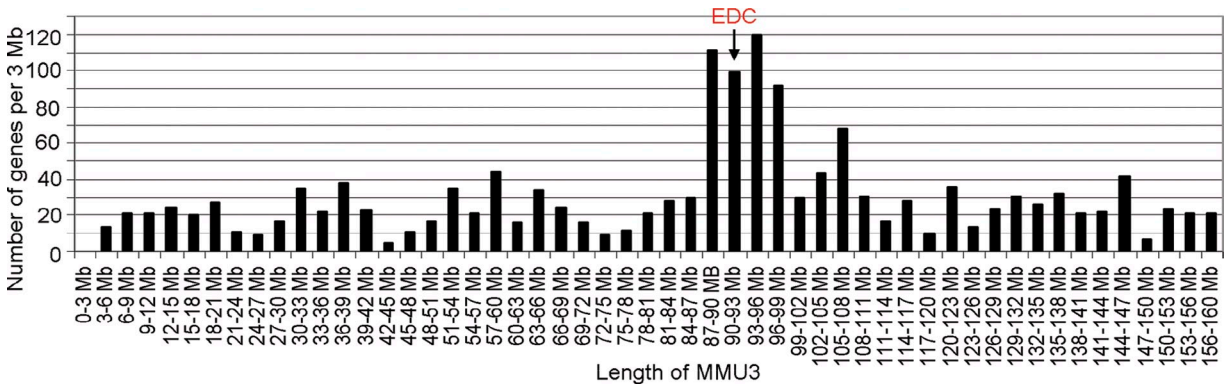

Figure S1. **EDC is located in the gene-dense region of mouse chromosome 3.** The data on the number of genes annotated to the distinct 3 Mb fragments of mouse chromosome 3 (arrow) were obtained from the National Center for Biotechnology Information Mouse Genome Bank.

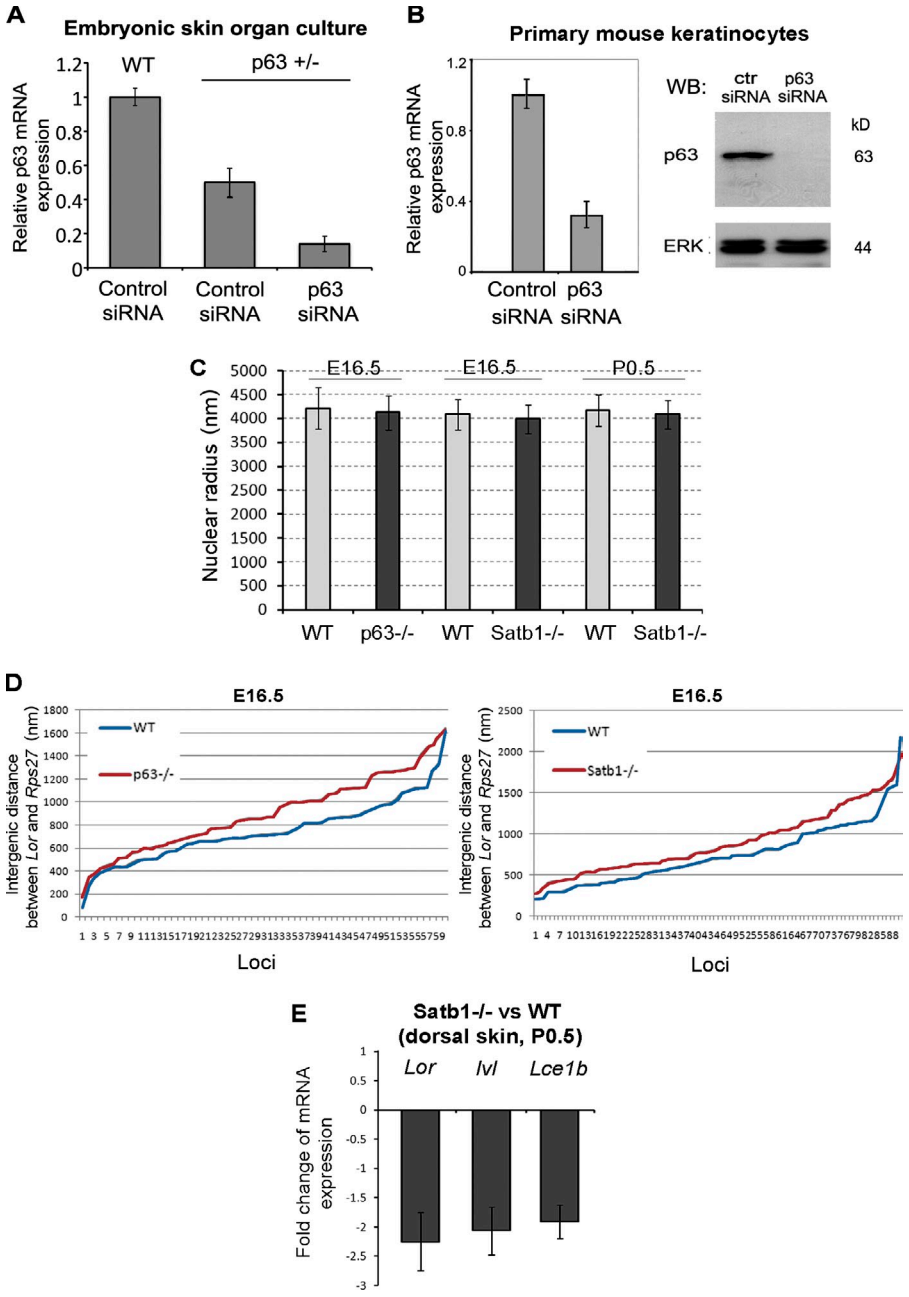

Figure S2. **Validation of the effects of p63 knockdown after siRNA treatment in skin explants and keratinocytes as well as the data on the analyses of 3D FISH distances and gene expression in the epidermis of p63$^{-/-}$, Satb1$^{-/-}$, and corresponding WT mice.** (A) Quantitative RT-PCR analysis of the p63 transcripts in E13.5 embryonic skin explants after treatment with p63 siRNA. Marked decrease of p63 transcripts in skin explants of heterozygous p63$^{+/-}$ mice after treatment with p63 siRNA versus the controls. Three samples were analyzed for each experimental group, and quantitative RT-PCR was run in triplicate for each sample. (B, right) A Western blot (WB) of p63 protein and real-time PCR of p63 transcripts in primary mouse keratinocytes treated by p63 siRNA for 48 h. ctr, control; ERK, extracellular signal-regulated kinase. (left) Decrease of p63 mRNA by ∼70% in cells treated by p63 siRNA versus the controls. Three independent experiments were run, and quantitative RT-PCR was run in triplicate for each sample in every experiment. (C) Lack of significant differences in the mean radius of the basal epidermal nuclei between p63$^{-/-}$, Satb1$^{-/-}$, and corresponding WT mice. 30–40 nuclei were analyzed for each experimental group. (D) Distribution of the 3D FISH distances (without normalization to the nuclear radius of each nucleus) between the *Rps27*and *Lor* in 60 loci of basal epidermal cells at E16.5 p63$^{-/-}$, Satb1$^{-/-}$, and corresponding WT mice. Individual loci are shown in the x axis. (E) Quantitative RT-PCR analyses of the distinct EDC genes in the epidermis of the dorsal skin of newborn Satb1$^{-/-}$ mice normalized to the expression levels in the corresponding WT mice. RNA samples were isolated from the dorsal skin of two Satb1$^{-/-}$ and two WT animals, and quantitative RT-PCR was run in triplicate for each RNA sample. (A–C and E) Error bars represent SEM.

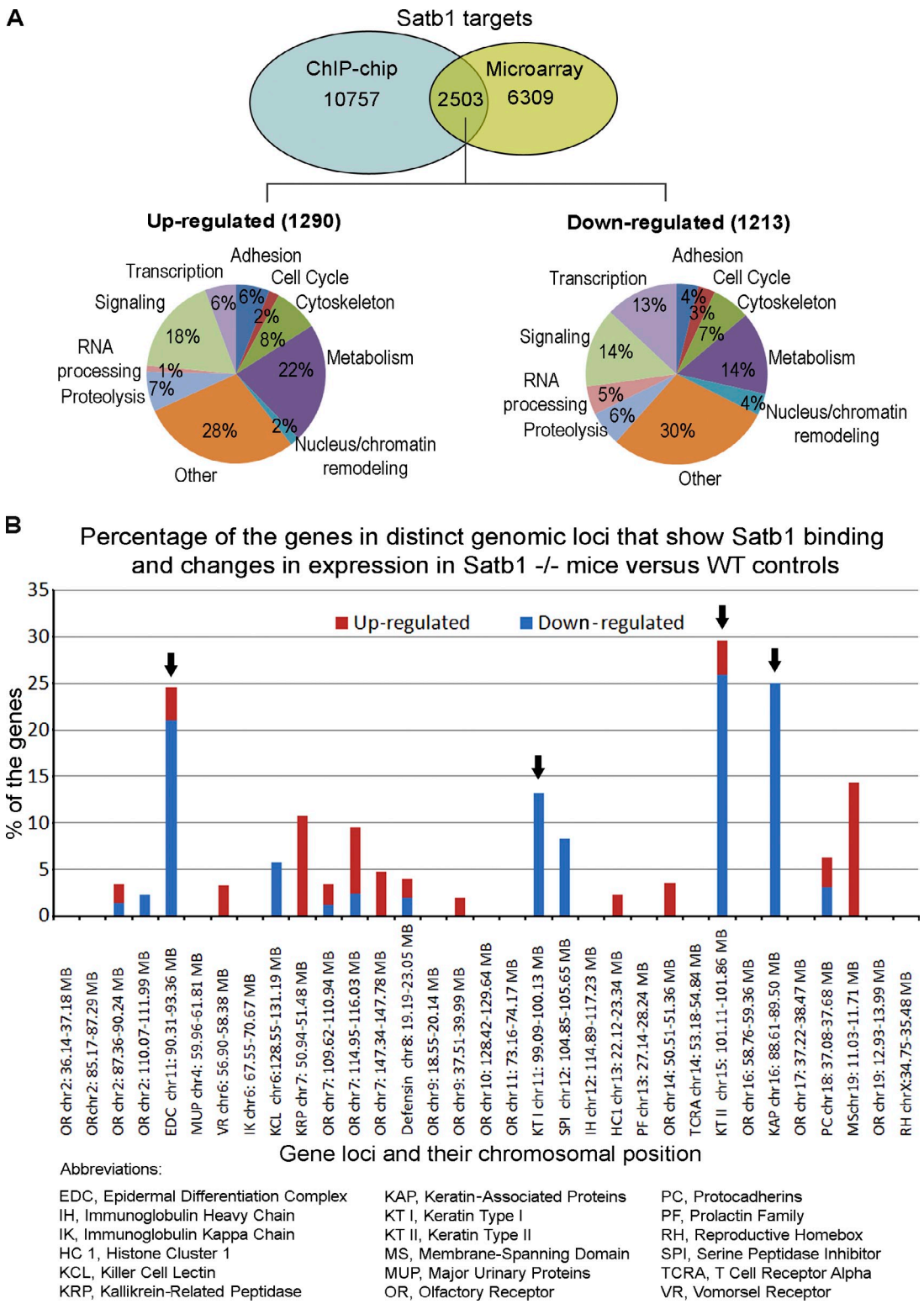

Figure S3. **Skin of newborn Satb1$^{-/-}$ and WT mice processed for RNA extraction and subsequent Agilent microarray and quantitative RT-PCR analyses.** Primary keratinocytes isolated from E16.5 or newborn skin were processed for ChIP-on-chip analysis with an antibody against the Satb1 or purified goat IgG. (A) Diagrams showing the ontology of the genes whose expression was altered in the skin of Satb1$^{-/-}$ mice versus WT controls and which showed association of Satb1 with the genomic regions within 200 kb from the transcription start sites in the ChIP-on-chip assay. (B) Bioinformatic analysis of the microarray data from the skin of Satb1$^{-/-}$ mice and ChIP-on-chip data with Satb1 antibody from primary mouse keratinocytes. Among 33 genomic loci >0.5 Mb containing functionally relevant genes, keratinocyte-specific loci (EDC, keratin type I/II loci, and keratin-associated protein locus; arrows) show significant ($P < 0.05$) enrichment of the genes that showed twofold or higher down-regulation of their expression in the skin of Satb1$^{-/-}$ mice compared with WT mice as well as Satb1 binding to genomic regions within 200 kb from the transcription start sites.

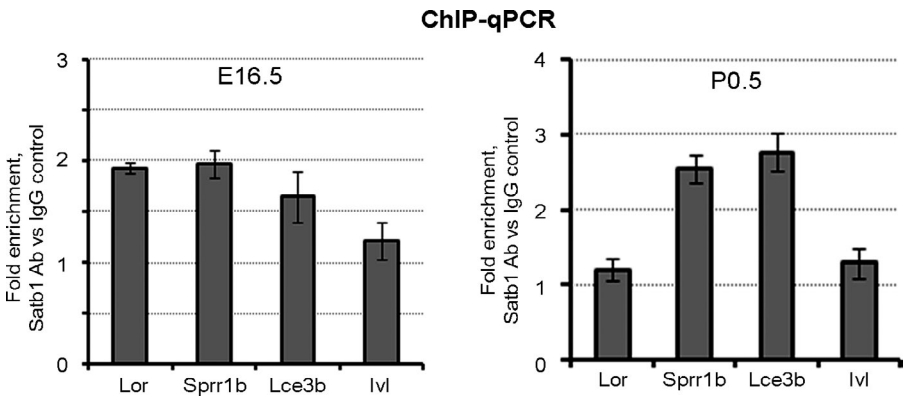

Figure S4. **Primary mouse keratinocytes (E16.5 and P0.5) processed for ChIP–quantitative PCR analyses with Satb1 antibody.** Quantitative RT-PCR analysis of the distinct promoter regions of the *Lor*, *Sprr1b*, *Lce3b*, and *Ivl* with primers listed in Table S9. Specific high-affinity binding of Satb1 to the promoters of the *Lor*, *Sprr1b*, and *Lce3b* genes ($P < 0.05$). Two independent ChIP experiments were run for each mouse developmental stage, and three quantitative RT-PCR experiments were run in triplicate to analyze DNA recovered after each ChIP. Error bars represent SEM.

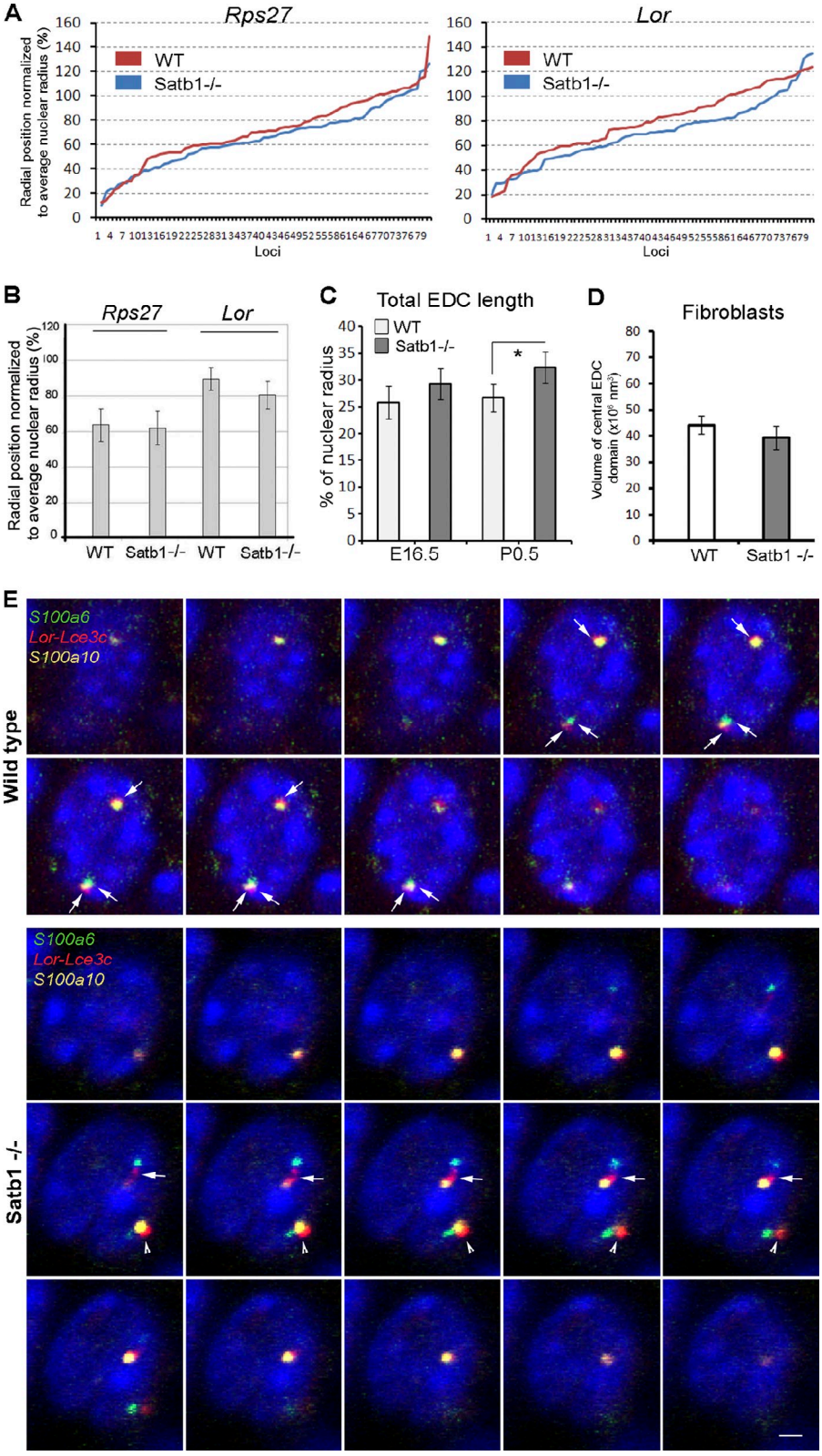

Figure S5. **Skin cryosections of P0.5 Satb1$^{-/-}$ and WT mice were processed for 3D FISH analyses of the EDC chromatin structure.** (A) Distribution of the radial positions of *Rps27*and *Lor* in 80 loci of basal epidermal cells of newborn Satb1$^{-/-}$ and WT mice. Because of the ellipsoid shape of the nuclei, radial positions of the genes in some nuclei are longer compared with the mean nuclear radius. Individual loci are shown in the x axis. (B) Relative radial position of *Lor* and *Rps27* normalized to the mean radius of each nuclei in basal epidermal keratinocytes of WT and Satb1$^{-/-}$ mice (P0.5; mean ± SEM, *n* = 80). Pairwise comparisons represent the lack of significant differences between the WT versus Satb1$^{-/-}$ mice (P > 0.05, Newman–Keuls test after a one-way ANOVA test). (C) Significant increase of the total EDC length normalized to the mean radius of the nuclei in basal epidermal cells of WT and Satb1$^{-/-}$ mice at P0.5 compared with E16.5 (mean ± SEM, *n* = 70; *, P > 0.05, Newman-Keuls test after a one-way ANOVA test). (D) Statistical analysis shows lack of differences in the volume of the central EDC domain in dermal cells of Satb1$^{-/-}$ mice compared with that of WT mice. The volume of the central EDC domain was determined in the fibroblasts of two Satb1$^{-/-}$ and two WT mice; 30 nuclei (60 alleles) were analyzed in each animal. Error bars represent SEM. (E) 3D FISH with probes depicting the 5′ and 3′ ends of the EDC (*S100a6* and *S100a10* genes) and the central domain (*Lor-Lce3c*) in the basal epidermal cells of Satb1$^{-/-}$ and WT mice. Each image is a 2D representation of 3D image stacks of 0.2-µm z sections. The central EDC domains of the distinct alleles are shown by arrows and arrowheads. Bar, 2 µm.

Tables S1–S10 are available as a separate file.

Table S1 shows genes down-regulated in the skin epithelium of the E16.5 p63$^{-/-}$ versus WT mice.

Table S2 shows genes up-regulated in the skin epithelium of the E16.5 p63$^{-/-}$ versus WT mice.

Table S3 shows 3D FISH BAC probes generated to the distinct regions of mouse chromosome 3.

Table S4 lists genes that show Satb1 binding to their regulatory regions and that are down-regulated in the skin of the P0.5 Satb1$^{-/-}$ versus WT mice.

Table S5 lists genes that show Satb1 binding to their regulatory regions and that are up-regulated in the skin of the P0.5 Satb1$^{-/-}$ versus WT mice.

Table S6 shows SATB1-binding sites in the EDC locus and its 5' and 3' flanking regions based on the ChIP-on-chip analysis.

Table S7 shows the length of the distinct EDC domains in Satb1$^{-/-}$ and WT mice.

Table S8 shows a list of the primers for quantitative RT-PCR.

Table S9 shows a list of the primers for the PCR analysis after ChIP.

Table S10 shows a list of primary antibodies.